Finite-volume Methods for the Solution of Partial Differential Equations

Luciano Rezzolla

Institute for Theoretical Physics,
Frankfurt, Germany

October 13, 2018

Contents

Chapter 1

Introduction

A system of equations is in conservative form if it can be written as

$$\mathbf{U}_t + \mathbf{F}(\mathbf{U})_x = 0, \tag{1.1}$$

with initial and boundary conditions given by

$$\mathbf{U}(x,0) = \mathbf{U}^{(0)}(x), \tag{1.2}$$
$$\mathbf{U}(0,t) = \mathbf{U}_L(t), \tag{1.3}$$
$$\mathbf{U}(1,t) = \mathbf{U}_R(t), \tag{1.4}$$

where $\mathbf{U}$ is the vector of conserved variables, while $\mathbf{F}(\mathbf{U})$ is the vector of fluxes. $\mathbf{U}^{(0)}(x)$ is the initial data at $t = 0$; $[0, 1]$ is the spatial domain and boundary conditions are assumed to be represented by the boundary functions $\mathbf{U}_L(t)$ and $\mathbf{U}_R(t)$.

The use of a conservative form of the equations is particularly important when dealing with problems admitting shocks or other discontinuities in the solution. A non-conservative numerical method, i.e. a numerical method in which the equations are not written in a conservative form, might give a numerical solution which looks reasonable but is incorrect. A well known example is provided by Burger's equation, i.e. the momentum equation of an isothermal gas in which pressure gradients are neglected, and whose non-conservative representation fails dramatically in providing the correct shock speed if the initial conditions contain a discontinuity (see Leveque 1992, [8]). As proved by Hou & Le Floch (1994) [6], non conservative schemes do not converge to the correct solution if a shock wave is present in the flow, whereas, as Lax & Wendroff (1960) [7] showed in a classical paper, conservative numerical methods, if convergent, do converge to the *weak solution* of the problem. On the other hand, it should be remembered that a conservative formulation and a non-conservative one are equivalent as long as the solution remains smooth.

1.1 Conservation form of the 1D Euler equations

The Newtonian hydrodynamics equations for a one-dimensional, non self-gravitating fluid

$$\frac{\partial \rho}{\partial t} + \frac{\partial (\rho u)}{\partial x} = 0 \,, \tag{1.5}$$

$$\frac{\partial (\rho u)}{\partial t} + \frac{\partial (\rho u^2 + p)}{\partial x} = 0 \,, \tag{1.6}$$

$$\frac{\partial E}{\partial t} + \frac{\partial [u(E+p)]}{\partial x} = 0 \,, \tag{1.7}$$

$$\tag{1.8}$$

offer a simple example of a system of equations that can be written in conservative form like in (1.1) with a vector of conserved variables given by

$$\mathbf{U} = \begin{bmatrix} \rho \\ \rho u \\ E \end{bmatrix} \tag{1.9}$$

and a flux given by

$$\mathbf{F} = \begin{bmatrix} \rho u \\ \rho u^2 + p \\ u(E+p) \end{bmatrix} \,, \tag{1.10}$$

where $E = \frac{1}{2}\rho u^2 + \rho\epsilon$ is the total energy, ϵ the specific internal energy. In the case of the Euler equations the conservative formulation reflects the physical conservation of specific and well defined quantities, i.e. the mass, the momentum and the energy. However, for other system of equations it may happen that the conservative formulation does not reflect any true conserved physical quantity.

1.2 Integral Form of Conservation Laws

Consider a one-dimensional time dependent system described by the Euler equations written in conservation laws. We can now discretize the spatial domain into N computing cells $I_i = [x_{i-1/2}, x_{i+1/2}]$ of size $\Delta x = x_{i+1/2} - x_{i-1/2}$, with $i = 1, ..., N$. We also define a "control volume" as $V \equiv I_i \times [t^n, t^{n+1}]$ (see Fig. 1.1).

The integral form of the conservative equations (1.1) on this domain can be written by first integrating (1.1) in space over I_i

$$\frac{d}{dt}\int_{x_{i-1/2}}^{x_{i+1/2}} \mathbf{U}(x,t)dx = \mathbf{F}(\mathbf{U}(x_{i-1/2},t)) - \mathbf{F}(\mathbf{U}(x_{i+1/2},t)) \,, \tag{1.11}$$

and then in time between t^n and t^{n+1}, with $t^n < t^{n+1}$ to obtain

$$\begin{aligned} \int_{x_{i-1/2}}^{x_{i+1/2}} \mathbf{U}(x,t^{n+1})dx \quad = \quad & \int_{x_{i-1/2}}^{x_{i+1/2}} \mathbf{U}(x,t^n)dx + \\ & \int_{t^n}^{t^{n+1}} \mathbf{F}(\mathbf{U}(x_{i-1/2},t))dt - \int_{t^n}^{t^{n+1}} \mathbf{F}(\mathbf{U}(x_{i+1/2},t))dt \,, \end{aligned} \tag{1.12}$$

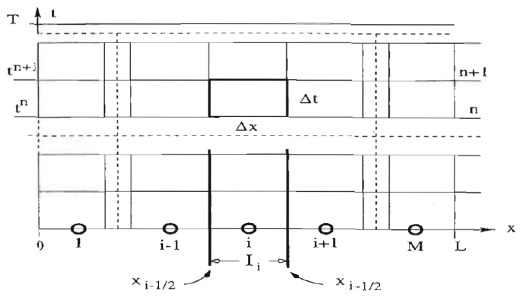

Figure 1.1: Mesh.

which represents the integral form of the equations. At this point we define two new quantities

$$\mathbf{U}_i^n = \frac{1}{\Delta x}\int_{x_{i-1/2}}^{x_{i+1/2}} \mathbf{U}(x,t^n)dt \tag{1.13}$$

and

$$\mathbf{F}_{i\pm 1/2} = \frac{1}{\Delta t}\int_{t^n}^{t^{n+1}} \mathbf{F}[\mathbf{U}(x_{i\pm 1/2},t)]dt \tag{1.14}$$

such that (1.12) is re-written as

$$\mathbf{U}_i^{n+1} = \mathbf{U}_i^n + \frac{\Delta t}{\Delta x}(\mathbf{F}_{i-1/2} - \mathbf{F}_{i+1/2}). \tag{1.15}$$

Important remarks:

- (1.15) is not yet a numerical scheme. In fact, it has been obtained through mathematical definitions with no approximations. One should in fact distinguish between the mathematical formulation of the method, which assumes the knowledge of the analytic functions $\mathbf{U}(x,t)$ and $\mathbf{F}(x,t)$, from its numerical application, which requires an interpretation of the terms entering (1.15) before a numerical scheme is effectively built.
- (1.15) becomes a numerical scheme, and indeed it is called "Godunov scheme", when approximation are introduced for the computations of the numerical fluxes $\mathbf{F}_{i-1/2}$ and an interpretation is given to the averages $\mathbf{U}_i$.
- In Godunov's *first order method* the evolution from the time t^n to the time $t^{n+1} = t^n + \Delta t$ is obtained by first assuming a *piece-wise* constant distribution of the data over the spatial grid, i.e. by assuming that $\mathbf{U}_i$ are constant (see Fig.1.2). Of course, by doing so, part of the knowledge of the original initial data $\mathbf{U}(x,t^n)$ inside the cell is lost, and to increase the spatial accuracy a number of reconstruction procedures has been developed.

- Different numerical algorithms can then be devised from (1.15) according to the method used to calculate the fluxes at each interface, $\mathbf{F}_{i-1/2}$ and $\mathbf{F}_{i+1/2}$. At the interface between adjacent numerical cells the quantity $\mathbf{U}_i$ manifests a jump, thus generating a sequence of local Riemann problems. Hence, we say that (1.15) is *Godunov's first-order upwind method* if the fluxes are calculated by solving such sequence of local Riemann problems. The left and right states are the same piece wise constant distribution of data given by (1.13). Solving the local Riemann problem provides either the term $\mathbf{U}(x_{i\pm1/2}, t)$ to be used in (1.14), or the $\mathbf{F}[\mathbf{U}(x_{i\pm1/2}, t)]$ term itself.

- Finally, it should be recalled that the Godunov scheme (1.15) with the piece wise constant distribution of the data is just first order accurate in time and space. This can be better appreciated if we apply the scheme (1.15) to the linear advection equation with the flux given by $\mathbf{F} = \lambda\mathbf{U}$. In this case the solution of each local Riemann problem at the generic cell interface $x_{i+1/2}$ is given by $\mathbf{U}_i^n$, if $\lambda < 0$, and by $\mathbf{U}_{i+1}^n$, if $\lambda > 0$. Therefore, the resulting scheme is given by

$$\mathbf{U}_i^{n+1} = \mathbf{U}_i^n - c(\mathbf{U}_i^n - \mathbf{U}_{i-1}^n), \qquad \text{if } \lambda > 0, \tag{1.16}$$

  and

$$\mathbf{U}_i^{n+1} = \mathbf{U}_i^n - c(\mathbf{U}_{i+1}^n - \mathbf{U}_i^n), \qquad \text{if } \lambda < 0, \tag{1.17}$$

  where $c = \lambda\Delta t/\Delta x$ is the *Courant factor*. The schemes (1.16) and (1.17) are nothing but *the first order upwind* method first introduced by Courant *et al.* (1952). The spatial accuracy of the first order Godunov's method presented here can be improved by adopting some kind of reconstruction procedure, while the time accuracy can be increased by combining the method outlined above with a conservative Runge-Kutta scheme.

- A final remark about the scheme (1.15) is that the time step Δt must satisfy a Courant-Friedrich-Lewy type condition (Courant *et al.* 1928)

$$\Delta t \leq \frac{\Delta x}{|v_{\max}^n|}, \tag{1.18}$$

  where $v_{\max}^n$ denotes the maximum wave velocity[1] present through the computational domain at time t^n.

It should be emphasized that the originality of Godunov's idea consists of the way an upwind method is obtained for a general nonlinear system of equations. Upwind methods, we recall, are characterized by the fact that the spatial differencing is performed using grid points on the side from which information flows. If we think of the advection equation as modelling the advection of a concentration profile in a fluid stream, then this is exactly the upwind direction. For a linear system of equations, upwind methods can only be used if all the eigenvalues of the matrix $\mathbf{F}$ have the same sign.

[1] Note that in a Riemann problem both shock waves and rarefaction waves are produced, so one has to look for the fastest wave at each time step. In multidimensional problems, when this procedure might become unsuitable, a common alternative is to select v_{max}^n as $v_{\max}^n = max(|v_i^n| + a_i^n)$, where v_i^n is the flow velocity and a_i^n is the sound speed.

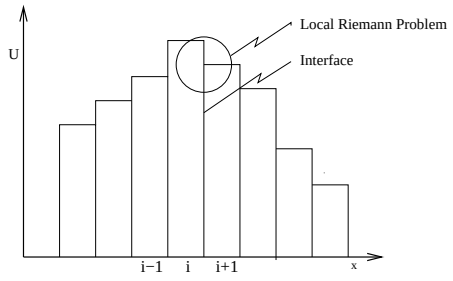

Figure 1.2: Schematic representation of a piece-wise constant distribution of a general quantity $\mathbf{U}$ giving rise to a sequence of local Riemann problems at the interface between adjacent cells.

If the eigenvalues have mixed signs, an alternative procedure is often adopted aimed at identifying the direction of propagation of information on the numerical grid. According to this procedure, the flux $\mathbf{F}$ is decomposed in two parts, $\mathbf{F}^+$ and $\mathbf{F}^-$, in such a way that the corresponding Jacobian matrices $\mathbf{F}^+ = \partial\mathbf{F}^+/\partial\mathbf{U}$ and $\mathbf{F}^- = \partial\mathbf{F}^-/\partial\mathbf{U}$ contain just the positive and negative eigenvalues, respectively, of the original matrix $\mathbf{F}$. The upwind character of the resulting numerical methods, called Flux Vector Splitting methods (FVS), is thus guaranteed. However, for nonlinear systems of equations the matrix of eigenvectors is not constant, and this same approach does not apply directly. Godunov succeeded in obtaining an upwind method in which the local characteristic structure is not provided by diagonalizing the Jacobian matrix, but rather by solving a Riemann problem forward in time. The solutions of Riemann problems, in fact, provide the necessary information about the characteristic structure, and lead to conservative methods, since they are themselves solution of the conservation laws.

Chapter 2

Approximate Riemann solvers for the Euler equations

Godunov's method, and its higher order modifications, require the solution of the Riemann problem at every cell boundary and on each time level. This amounts to calculating the solution in the regions that form behind the non-linear waves developing in the Riemann problem (as shown in Fig. 2.1) as well as the wave speeds necessary for deriving the complete wave structure of the solution.

The solution of the general Riemann problem cannot be given in a closed analytic form, even for one dimensional Newtonian flows. What can be done is to find the answer numerically to any required accuracy, and in this sense the Riemann problem is said to have been solved *exactly*, even though the actual solution is not analytical. In Newtonian hydrodynamics, the exact solution of the one dimensional Riemann problem was found by Courant & Friedrichs (1948).

Approximate Riemann solvers can be divided in *approximate State* Riemann Solvers, where an approximation is given to the state $\mathbf{U}(x_{i\pm1/2}, t)$ which is then used to evaluate the corresponding flux by (1.14), and in *approximate Flux* Riemann Solvers, where an approximation is given to the flux directly, thus avoiding the computation of the state $\mathbf{U}(x_{i\pm1/2}, t)$ at each zone edge.

2.1 Approximate State Riemann Solvers

2.1.1 "Two-Rarefactions" Riemann Solver

Finding the wave pattern in a Riemann problem is part of the solution procedure, but if one assumes a priori that both nonlinear waves are rarefactions, then the solution can be obtained analytically (see Toro (1997) for the Newtonian case and [11] for the relativistic case). The resulting method is very accurate for flow conditions near vacuum, when rarefaction waves give indeed the best approximation to the problem.

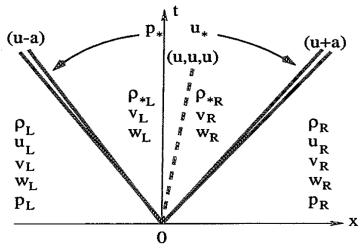

Figure 2.1: Riemann problem for the 3D Euler equation: **u** is the fluid speed, **a** is the sound speed. The 1D case can be recovered simply disregarding the tangential velocities in the y and z direction v and w starting from an initial condition in which they are zero on both sides of the discontinuity. The variables ρ and p represent density and pressure respectively.

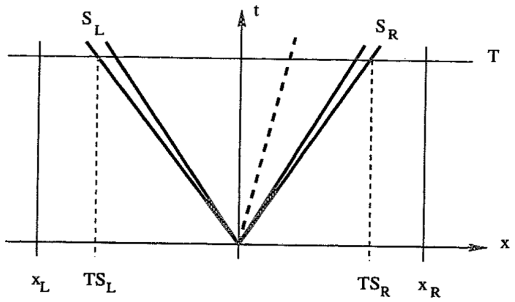

Figure 2.2: Control volume for the computation of the approximate HLLE flux.

2.1.2 "All-Shocks" Riemann Solver

In analogy with the previous solver, it is possible to ignore the occurrence of rarefaction waves and assume that both nonlinear waves are shock waves. This represents a good approximation in a wide range of flow conditions, particularly when dealing with more complicated equations of state than the usual polytropic one (see Colella, 1982). However, this approach is typically inadequate in the case of a transonic rarefaction, yielding a numerical solution which does not satisfy the entropy condition.

2.2 Approximate Flux Riemann Solvers

2.2.1 The HLL(E) Solver

In the Riemann solver given by Harten, Lax and van Leer (1983) and later improved by Einfeldt (1988), ie the HLLE approximate-flux Riemann solver or simply HLLE Riemann solver, it is assumed that, after the decay of the initial discontinuity of the local Riemann problem, only two waves propagate in two opposite directions with

velocities S_L and S_R, generating a single state between them, i.e.

$$\mathbf{U} = \begin{cases} \mathbf{U}_L & \text{if} \quad x/t < S_L, \\ \mathbf{U}^{\text{HLLE}} & \text{if} \quad S_L < x/t < S_R, \\ \mathbf{U}_R & \text{if} \quad x/t > S_R, \end{cases}$$

where S_L and S_R are the smallest and the largest of the signal speeds arising from the solution of the Riemann problem[1].

We will now show how to compute $\mathbf{U}^{\text{HLLE}}$. The time integral form of Eq. (1.10 on the control volume defined in Fig. 2.2 is:

$$\int_{x_L}^{x_R} \mathbf{U}(x,T)dx = \int_{x_L}^{x_R} \mathbf{U}(x,0)dx + \int_0^T \mathbf{F}(\mathbf{U}(x_L,t))dt - \int_0^T \mathbf{F}(\mathbf{U}(x_R,t))dt. \tag{2.1}$$

The evaluation of the right-hand side gives a *consistency condition*:

$$\int_{x_L}^{x_R} \mathbf{U}(x,T)dx \quad = \quad x_R\mathbf{U}_R - x_L\mathbf{U}_L + T(\mathbf{F}_L - \mathbf{F}_R) \tag{2.2}$$

where $\mathbf{F}_L = \mathbf{F}(\mathbf{U}_L)$ and $\mathbf{F}_R = \mathbf{F}(\mathbf{U}_R)$. Now we split the the integral on the left-hand side of Eq. (2.1) into three integrals

$$\int_{x_L}^{x_R} \mathbf{U}(x,T)dx = \int_{x_L}^{TS_L} \mathbf{U}(x,T)dx + \int_{TS_L}^{TS_R} \mathbf{U}(x,T)dx + \int_{TS_R}^{x_R} \mathbf{U}(x,T)dx$$

and evaluate the first and third terms on the right-hand side. We obtain:

$$\int_{x_L}^{x_R} \mathbf{U}(x,T)dx = \int_{TS_L}^{TS_R} \mathbf{U}(x,T)dx + (TS_L - x_L)\mathbf{U}_L + (x_R - TS_R)\mathbf{U}_R \tag{2.3}$$

Comparing Eq. (2.2) with Eq. (2.3) gives

$$\int_{TS_L}^{TS_R} \mathbf{U}(x,T)dx = T(S\mathbf{U}_R - S_L\mathbf{U}_L + \mathbf{F}_L - \mathbf{F}_R) \tag{2.4}$$

Dividing by the length $T(S_R - S_L)$ we finally obtain:

$$\mathbf{U}^{\text{HLLE}} = \frac{1}{T(S_R - S_L)} \int_{TS_L}^{TS_R} \mathbf{U}(x,T)dx = \frac{(S\mathbf{U}_R - S_L\mathbf{U}_L + \mathbf{F}_L - \mathbf{F}_R)}{(S_{R-}S_L).} \tag{2.5}$$

Thus the integral average of the exact solution of the Riemann problem between the slowest and the fastest signals at time T is a known constant, provided that the signal

[1]The simplest choice is to take the smallest and the largest among the eigenvalues of the Jacobian matrix $\partial\mathbf{F}/\partial\mathbf{U}$ evaluated at some intermediate state. For the 1D Euler equation the simplest estimate proposed by Davis in [12] would be $S_L = u_l - a_l$ and $S_R = u_r + a_r$, where the u's are the fluid velocities and the a's the sound speeds on the left and on the right of the initial discontinuity respectively.

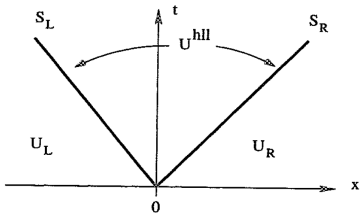

Figure 2.3: Approximate state for HLLE: the integral average of the exact solution of the Riemann problem between the slowest and the fastest signals at a given time T is a known constant, provided that the signal speeds S_L and S_R are known; such constants is the right-hand side of Eq. (2.5).

speeds S_L and S_R are known; such constants is the right-hand side of Eq. (2.5) and we denote it by

$$\mathbf{U}^{\text{HLLE}} = \frac{S_R\mathbf{U}_R - S_L\mathbf{U}_L + \mathbf{F}_L - \mathbf{F}_R}{S_R - S_L} \tag{2.6}$$

We now apply the Rankine-Hugoniot conditions (see Appendix 4) across the left and the right waves, to obtain

$$\mathbf{F}^{\text{HLLE}} = \mathbf{F}_L + S_L(\mathbf{U}^{\text{HLLE}} - \mathbf{U}_L) \tag{2.7}$$

$$\mathbf{F}^{\text{HLLE}} = \mathbf{F}_R + S_R(\mathbf{U}^{\text{HLLE}} - \mathbf{U}_R) \tag{2.8}$$

Finally, by replacing (2.6) into (2.7) or into (2.8) we obtain the HLLE flux to be used in the Godunov scheme

$$\mathbf{F}^{\text{HLLE}} = \frac{S_R\mathbf{F}_L - S_L\mathbf{F}_R + S_LS_R(\mathbf{U}_R - \mathbf{U}_L)}{S_R - S_L}. \tag{2.9}$$

This Riemann solver, which is very simple in its original form, performs well at critical sonic rarefactions but produces excessive smearing at contact discontinuities due to the fact that middle waves are ignored in the solution. Furthermore, it needs to be implemented with an algorithm for the calculation of the wave speeds S_L and S_R.

Chapter 3

High-Resolution Shock Capturing Methods

A large effort has been spent in recent years in developing a numerical method able to satisfy the following requirements

- at least second order accuracy on smooth parts of the solution,
- sharp resolution of discontinuities without large smearing,
- absence of spurious oscillations everywhere in the solution,
- converge to the "true" solution as the grid is refined.

Irrespective of the Riemann solver adopted, the original Godunov method is only first order accurate on smooth solutions and gives poor approximations to shock waves and other discontinuities. However, if we wanted to modify the first order Godunov method in order to obtain a higher order numerical scheme we would encounter a fundamental difficulty. Namely, all higher order linear schemes produce nonphysical oscillations in the vicinity of large gradients. If we define a *monotone* linear scheme of the form $u_i^{n+1} = H(u_{i-l}^n, ..., u_{i+r}^n)$, where H is a linear operator, as a scheme for which $\partial H/\partial u_k^n \geq 0$ for all k, then only monotone linear schemes do not suffer from oscillations. Unfortunately, as proved by Godunov (1959), monotone schemes are at most first order accurate. As a result, higher order linear schemes and absence of oscillations are two incompatible requirements, forcing the use of nonlinear numerical methods. To summarize: HRSC methods result from the combination of Godunov type methods, which take advantage of the conservation form of the equations, and of numerical techniques aimed at obtaining second order (or higher) accuracy in smooth parts of the solution without producing oscillations.

3.1 Total Variation Diminishing Methods

The concept of spurious oscillations in the solution can be made more quantitative by the notion of the *total variation* of the solution. The total variation of a grid function Q at time level t^n is defined as

$$TV(Q^n) \equiv \sum_{i=-\infty}^{+\infty} |Q_i^n - Q_{i-1}^n|, \tag{3.1}$$

and is used to "measure" the oscillations appearing in a numerical solution. The requirement to have a scheme that is both second (or higher) order accurate and does not produce spurious oscillations is that the total variation should not be increasing in time, so that the total variation at any time is uniformly bounded by the total variation of the initial data. In other words, a numerical method is said to be *total variation diminishing* (TVD) if, for any set of data Q^n, the values Q^{n+1} computed by the method satisfy

$$TV(Q^{n+1}) \leq TV(Q^n). \tag{3.2}$$

TVD schemes are intimately linked to the more traditional Artificial Viscosity methods (see Richtmyer & Morton, 1967), where viscous terms were introduced explicitly in the scheme in order to eliminate or at least control the appearance of the oscillations. In modern TVD methods, on the contrary, artificial viscosity is inherent to the scheme itself in a rather sophisticated way. TVD methods do not generally extend beyond second order accuracy. To construct third (and higher) order methods one must drop condition (3.2) and allow for an increase of the total variation which is proportional to some power of the typical step size. The resulting methods are called Essentially Non-Oscillatory (ENO) (see Toro, 1997).

3.2 Reconstruction Procedures

Due to the discrete numerical representation, any information about the behavior of the quantities inside the numerical cell is lost. In order to recover in part this information and improve the spatial accuracy of a numerical code based on Riemann solvers, different spatial reconstruction procedures have been developed. The common goal is to interpolate the profiles of the various thermodynamical quantities within each cell, thus providing a better estimate for the calculation of the left and of the right state of the Riemann problem to be solved at the interface between two adjacent cells.

Van Leer (1979) was the first to introduce the idea of modifying the piece-wise constant data (1.13) as a first step in achieving higher order spatial accuracy. This approach has been generically called Monotone Upstream-centered Scheme for Conservation Laws (MUSCL). Since then, many other reconstruction procedures have been developed, such as the piece-wise parabolic method (PPM) of Colella & Woodward (1984), or the piece-wise hyperbolic (PHM) method of Marquina (1994), where the interpolation is obtained by using hyperbolae instead of parabolae.

Chapter 4

Appendix: Rankine-Hugoniot condition

The integral form of Eq. (1.1) on the interval $[x_L, x_R]$ at time t is

$$\frac{d}{dt}\int_{x_L}^{x_R} \mathbf{U}(x,t)dx = \mathbf{F}(\mathbf{U}(x_L,t)) - \mathbf{F}(\mathbf{U}(x_R,t)) \tag{4.1}$$

We recall a simple formula to compute the derivative of an integral:

$$\frac{d}{dt}\int_{x_1(t)}^{x_2(t)} f(x,t)dx = \int_{x_1(t)}^{x_2(t)} \frac{\partial f(x,t)}{\partial t}dx + f(x_2(t),t)\frac{dx_2(t)}{dt} - f(x_1(t),t)\frac{dx_1(t)}{dt}. \tag{4.2}$$

If a discontinuity is present in the solution (see Fig. 2.2) and propagating along $s(t)$ we can split the left-hand side of Eq. (4.1) in the following way:

$$\frac{d}{dt}\int_{x_L}^{s(t)} \mathbf{U}(x,t)dx + \frac{d}{dt}\int_{s(t)}^{x_R} \mathbf{U}(x,t)dx = \mathbf{F}(\mathbf{U}(x_L,t)) - \mathbf{F}(\mathbf{U}(x_R,t)) \tag{4.3}$$

Applying formula (4.2) to Eq. (4.3) gives:

$$\mathbf{F}(\mathbf{U}(x_L,t))-\mathbf{F}(\mathbf{U}(x_R,t)) = [\mathbf{U}(s_L,t)-\mathbf{U}(s_R,t)]S+\int_{x_L}^{s(t)} \frac{\partial \mathbf{U}(x,t)}{\partial t}dx+\int_{s(t)}^{x_R} \frac{\partial \mathbf{U}(x,t)}{\partial t}dx \tag{4.4}$$

where $S = \frac{ds(t)}{dt}$ and $\mathbf{U}(s_L,t)$ and $\mathbf{U}(s_R,t)$ are the left and right limit of $\mathbf{U}(x,t)$ for $x \to s(t)$.

When $x_L \to s(t)$ and $x_R \to s(t)$ the two integrals on the right-hand side of Eq. (4.4) vanish and we finally obtain the Rankine-Hugoniot condition

$$\mathbf{F}(\mathbf{U}(s_L,t)) - \mathbf{F}(\mathbf{U}(s_R,t)) = [\mathbf{U}(s_L,t) - \mathbf{U}(s_R,t)]S \tag{4.5}$$

which connects states and fluxes across a discontinuity.

Bibliography

[1] Colella, P., 1982, SIAM J. Sci. Stat. Comput., 3, 76.

[2] Courant, R., Friedrichs, K. O., Lewy, H., 1928, Math. Ann., 100, 32

[3] Courant, R., Isaacson, E., Rees, M., 1952, Comm. Pure Appl. Math., 5, 243.

[4] Einfeldt, B., 1988, SIAM J. Num. Anal., 25, 294.

[5] Harten, A., Lax, P. D., van Leer, B., 1983, SIAM Reviews, 25, 35.

[6] Hou, T. Y., LeFloch, P., 1994, Math. of Comput., 62, 497.

[7] Lax, P. D., Wendroff, B., 1960, Comm. Pure Appl. Math., XVII, 381.

[8] Leveque, R. J. 1992, *Numerical Methods for Conservation Laws*, Birkhauser

[9] Leveque, R. J., Mihalas, D., Dorfi, E. A., Müller, E., 1998, *Computational Methods for Astrophysical Fluid Flows* Saas-Fee Advanced Course 27, Springer

[10] Martí, J.M. & Müller, E. 1994, J. Fluid Mech., 258, 317.

[11] Rezzolla, L. & Zanotti, O. 2001, J. Fluid Mech. 449, 395.

[12] S. F. Davis, SIAM J.Sci.Stat.Comput.,9:445-473,1988

[13] Toro, E. 1997, *Riemann Solvers and Numerical Methods for Fluid Dynamics*, Springer.